

**When to biopsy Prostate Imaging and Data Reporting System version 2 (PI-RADSv2) assessment category 3 lesions? Use of clinical and imaging variables to predict cancer diagnosis at targeted biopsy**

Christopher Lim<sup>1</sup>; Jorge Abreu-Gomez<sup>1</sup>; Michel-Alexandre Leblond<sup>1</sup>; Ivan Carrion<sup>1</sup>; Danny Vesprini<sup>2</sup>; Nicola Schieda<sup>3</sup>; Laurence Klotz<sup>4</sup>

<sup>1</sup>Department of Medical Imaging, Sunnybrook Health Sciences Centre, University of Toronto, Toronto, ON, Canada; <sup>2</sup>Department of Radiation Oncology, Sunnybrook Health Sciences Centre, University of Toronto, Toronto, ON, Canada; <sup>3</sup>Department of Radiology, The Ottawa Hospital, The University of Ottawa, Ottawa, ON, Canada; <sup>4</sup>Division of Urology, Department of Surgery, Sunnybrook Health Sciences Centre, University of Toronto, Toronto, ON, Canada

**Cite as:** Lim C, Abreu-Gomez J, Leblond M-A, et al. When to biopsy Prostate Imaging and Data Reporting System version 2 (PI-RADSv2) assessment category 3 lesions? Use of clinical and imaging variables to predict cancer diagnosis at targeted biopsy. *Can Urol Assoc J* 2020 September 28; Epub ahead of print. <http://dx.doi.org/10.5489/cuaj.6781>

Published online September 28, 2020

\*\*\*

**Abstract**

**Introduction:** We aimed to determine if clinical and imaging features can stratify men at higher risk for clinically significant (CS, International Society of Urological Pathology [ISUP] grade group  $\geq 2$ ) prostate cancer (PCa) in equivocal Prostate Imaging and Data Reporting System (PI-RADS) category 3 lesions on magnetic resonance imaging (MRI).

**Methods:** Approved by the institutional review board-approved, this retrospective study involved 184 men with 198 lesions who underwent 3T-MRI and MRI-directed transrectal ultrasound biopsy for PI-RADS 3 lesions. Men were evaluated including clinical stage, prostate-specific antigen density (PSAD), indication, and MRI lesion size. Diagnoses for all men and by indication (no cancer, any PCa, CSPCa) were compared using multivariate logistic regression, including stage, PSAD, and lesion size.

**Results:** We found an overall PCa rate of 31.8% (63/198) and 10.1% (20/198) CSPCa (13 grade group 2, five group 3, and two group 4). Higher stage ( $p=0.001$ ), PSAD ( $p=0.007$ ), and lesion size ( $p=0.015$ ) were associated with CSPCa, with no association between CSPCa and age, PSA, or prostate volume ( $p>0.05$ ). PSAD modestly predicted CSPCa area under the curve (AUC) 0.66 (95% confidence interval [CI] 0.518–0.794) in all men and 0.64 (0.487–0.799) for those on active surveillance (AS). Model combining clinical stage, PSAD, and lesion size improved

**Clinical and imaging variables to predict diagnosis at targeted biopsy**

accuracy for all men and AS (AUC 0.82 [0.736–0.910],  $p < 0.001$  and 0.785 [0.666–0.904],  $p < 0.001$ ). In men with prior negative biopsy and persistent suspicion, PSAD (0.90 [0.767–1.000]) was not different from the model ( $p > 0.05$ ), with optimal cutpoint of  $\geq 0.215$  ng/mL/cc achieving sensitivity/specificity of 85.7/84.4%.

**Conclusions:** PI-RADSv2 category 3 lesions are often not CSPCa. PSAD predicted CSPCa in men with a prior negative biopsy; however, PSAD alone had limited value, and accuracy improved when using a model incorporating PSAD with clinical stage and MR lesion size.

**Introduction**

PI-RADSv2 assessment categories positively correlate with an increased likelihood of detecting clinically significant prostate cancer (CSPCa) at targeted biopsy [1]. A PI-RADSv2 assessment category 3 (intermediate, clinically significant cancer likelihood equivocal) lesion is equivocal. Studies evaluating the likelihood of CSPCa cancer at targeted biopsy of PI-RADSv2 category 3 lesions have reported variable rates of PCa diagnosis, ranging from 5% to 30%, with the majority of studies showing a relatively low likelihood of eventual CSPCa diagnosis [2–4]. Management of PI-RADSv2 category 3 lesion is variable, ranging from immediate biopsy to surveillance [5, 6].

Given the disparity in management patterns for PI-RADSv2 3 lesions and a small but not insignificant proportion of these lesions harboring CSPCa, better classification of category 3 lesion is an unmet need. Previous studies in these patients have shown a correlation of CSPCa with older patient age, smaller prostate volumes, higher PSA density (PSAD) and increased clinical stage [7–11]. The purpose of this study was to evaluate a relatively large cohort of PI-RADSv2 category 3 lesions with histological confirmation to determine if clinical and imaging parameters could better delineate which category 3 lesion represent CSPCa and determine which patients should undergo targeted biopsy.

**Methods**

This retrospective study was approved by the local institutional review board, who waived the need for patient informed consent. Between the dates of January 1, 2015 and September 1, 2018, we searched our electronic Picture Archiving and Communications System (PACS) for all MRI-directed trans-rectal Ultrasound (TRUS) cognitive fusion targeted biopsies performed for category 3 lesion. 397 patients with 412 reported category 3 lesions were identified. An experienced radiologist (having interpreted over 750 MRI with PI-RADSv2) reviewed each MRI, blinded to histopathology results, and re-scored each lesion using PI-RADSv2 noting the location of each lesion using the using PI-RADSv2 sector map and using the peripheral zone (PZ) and transition zone (TZ) decision tree rules [12]. A total of 137 patients with 138 lesions

**Clinical and imaging variables to predict diagnosis at targeted biopsy**

were reclassified to a different PI-RADS categories and excluded, leaving 260 patients with 274 category 3 lesions. A total of 76 patients with 76 category 3 lesions were excluded due to inadequate imaging technique (i.e. without dynamic contrast enhancement, images with severe artifact [hip arthroplasties, rectal gas degrading image interpretation] etc.), prior treatment or presence of prostate cancer in a different location than the target lesion. A summary of patient inclusion and exclusion criteria are provided, Figure 1.

The clinical indication for MRI, patient age, PSA, prostate volume (measured on MRI using an ellipsoid volume calculation) and clinical stage (when available, recorded as T1c if there was negative digital rectal exam [DRE] and  $\geq$ T2 if positive DRE indicated by the referring physician) were recorded. PSAD was calculated by dividing the PSA by the MRI calculated total prostate volume. Biopsy results from MRI-TRUS fusion targeted biopsy including ISUP grade group were recorded.

***MRI technique and reporting***

During the study period, prostate MRI was performed using a 3-Tesla MRI system (Philips Ingenia, Amsterdam, the Netherlands). Details regarding the MRI protocols is summarized in Appendix 1. A standardized reporting template for prostate MRI was used.

***Targeted biopsy***

Targeted biopsies were performed using TRUS guidance with cognitive fusion of MRI data onto real time 2-Dimensional TRUS images. All ultrasound examinations were performed using modern ultrasound equipment (Phillips IU 22) and endocavity 5-9 Mhz end-fire probes. Biopsies were performed by a core-group of three fellowship trained abdominal radiologists with mean of 8.3 years of experience [range 3-15 years] in cognitive fusion targeted biopsy of the prostate.

The TRUS-guided biopsy system used for all biopsies employed an 18-gauge side-cutting needle. Biopsy were performed using standard technique as previous describe [13]. The cognitive fusion TRUS-guided biopsy reports specified: the target(s), the number of core biopsies performed per target (which is typically between 3-5 biopsies [14]) and the specimen container into which targeted biopsies are placed. In this way, a biopsy result for each targeted lesion can be extracted from the histopathology report, which was done by the blinded radiologist after review of MRI.

***MRI lesion size measurement***

The abdominal radiologist at time of initial database creation, blinded to other patient information and eventual histological diagnosis for each lesion, measured the size of lesion. For each lesion, the lesion was first classified as being located in either the PZ or TZ based upon the PI-RADSV2 sector map. For lesion that crossed two zones, the epicenter of the lesion was used to determine the primary zonal origin. There were no central zone lesion in this cohort. The radiologist measured the single longest transverse dimension on axial ADC map images for PZ

lesion and axial T2W for TZ lesion where the lesion appeared the largest as described in PI-RADSv2 [12], Figure 2.

To assess for reproducibility of measurements, an abdominal radiologist with seven years of experience in prostate MRI (BLINDED) measured the size of tumor in a randomly selected 20% of lesions, a previously described reliable proportion of lesion needed to determine reproducibility of measurements [15].

### ***Statistical analysis***

Categorical data were tabulated and parametric data presented as mean  $\pm$  standard deviation (with range). Comparisons were performed between category 3 lesions with a benign diagnosis and those with any PCa diagnosis and CSPCa diagnosis using multivariate logistic regression. Statistical analysis was performed using SPSS v26.0 (SPSS inc., IBM Corp.). Empiric ROC curves were constructed for each statistically significant variable associated with CSPCa and also for a logistic regression model combining statistically significant variables. Area under the ROC curve for each variable and for the logistic regression model were compared using ROC analysis and the optimal cutpoint which maximized sensitivity and specificity determined using the method described by Youden.

### **Results**

#### ***All patients***

Patient demographic and clinical data are presented in Table 1. The mean patient age, PSA and PSAD were  $63.36 \pm 8.43$  years,  $9.37 \pm 6.52$  (Range: 0.79-36.25) ng/mL and  $0.168 \pm 0.117$  (Range: 0.019-0.995) ng/mL/cc. A total of 81.0% (149/184) patients had clinical staging data from DRE available with 77.2% (115/149) negative or T1c and 22.8% (34/149)  $\geq$ T2a results.

From the 198 PI-RADSv2 category 3 MRI lesions, any PCa diagnosis was established in 32% (63/198) of biopsies, whereas, CSPCa was diagnosed in only 10% (20/198) of biopsies. Of the twenty CSPCa diagnoses, ISUP grade groups were: (ISUP 2, N=13; ISUP 3, N=5; ISUP 4, N=2). MRI lesions were fairly evenly split between the PZ and TZ, 54.0% (107/198) located in the PZ and 46.0% (91/198) located in the TZ; however, 30.0% (6/20) of CSPCa were located in the PZ and 70.0% (14/20) CSPCa were located in the TZ. The mean lesion size was  $12.7 \pm 5.4$  mm overall and  $11.1 \pm 4.2$  mm for lesions in the PZ and  $15.0 \pm 5.5$  mm for lesion in the TZ ( $p < 0.001$ ).

There was no association between age or PSA and CSPCa diagnosis ( $p=0.073$ ,  $0.591$  respectively); however, patients with any PCa diagnosis had lower PSA compared to those with benign histology ( $10.1 \pm 7.1$  versus  $7.9 \pm 5.0$  ng/mL,  $p=0.030$ ), Table 1. Both patients with any PCa and CSPCa diagnoses had higher clinical stage ( $p=0.027$  and  $0.001$ ) at DRE. Mean prostate volume was  $64.95 \pm 42.69$  (Range 18-324) mL. There was a trend with CSPCa diagnosis occurring in smaller prostate volumes ( $66.9 \pm 44.25$  mL versus  $49.1 \pm 21.4$  mL,  $p=0.078$ );

**Clinical and imaging variables to predict diagnosis at targeted biopsy**

however, the difference was not significant, Table 1. PSAD was significantly higher in patients with category 3 lesions which yielded CSPCa compared to patients with benign histology and any PCa diagnosis ( $0.234 \pm 0.151$  ng/mL/cc versus  $0.160 \pm 0.111$  ng/mL/cc,  $p=0.007$ ). Category 3 lesions which yielded any PCa and CSPCa were significantly larger ( $14.0 \pm 5.2$  mm and  $14.9 \pm 3.3$  mm versus  $12.4 \pm 5.2$  mm,  $p=0.047$  and  $0.015$ ) than those with benign histology. With respect to reproducibility of measurements, size measurements did not differ between observers ( $p=0.592$ ).

The area under the ROC curve (AUC) for the diagnosis of CSPCa using clinical stage, PSAD and, largest tumor size per patient evaluated independently were: 0.671 (95% Confidence Interval [CI] 0.529 - 0.812), 0.698 (0.570 - 0.826) and, 0.675 (0.582 - 0.768), respectively. A logistic regression model combining these three variables achieved an improved AUC for diagnosis of CSPCa diagnosis of 0.823 (0.737 - 0.910), ( $p<0.001$ ), Figure 3.

***Subgroup of men on active surveillance***

Subgroup analyses in men undergoing MRI performed for Active Surveillance (AS) are presented in Table 2. Notably, in MRI performed for AS, there was a trend towards CSPCa cancers having higher clinical stage; however, the results were not significant ( $p=0.056$ ). Category 3 lesions which yielded CSPCa were larger ( $p=0.028$ ). There was no association between PSAD and CSPCa ( $p=0.308$ ). In patients being evaluated on AS, AUCs for diagnosis of CSPCa using clinical stage, PSAD and, largest tumor size per patient were 0.637 (0.453 - 0.821), 0.643 (0.487 - 0.799), 0.701 (0.574 - 0.829), respectively. The logistic regression model combining all three features improved the AUC to 0.785 (0.666 - 0.904), ( $p<0.001$ ), Figure 4.

***Subgroup of on men with prior negative template biopsy and persistent suspicion***

Data on men undergoing MRI with prior negative template biopsy but persistent clinical suspicion of PCa are presented in Table 3. Notably, patients with CSPCa had higher PSAD and clinical stage at DRE ( $p=0.0001$ ,  $p=0.007$ ). There was no association between size and CSPCa ( $p=0.688$ ). In men undergoing MR for prior negative biopsy but persisting clinical suspicion of cancer, AUCs for diagnosis of CSPCa using clinical stage, PSAD and largest tumor size per patient were 0.708 (0.482 - 0.934), 0.898 (0.805 - 0.991), 0.605 (0.470 - 0.739), respectively. The logistic regression model combining all three variables achieved an AUC of 0.892 (0.767 - 1.000), which was not improved compared to PSAD alone ( $p>0.05$ ), Figure 5. The optimal cut-point which maximized the diagnostic accuracy for CSPCa diagnosis in this cohort of men was  $\geq 0.215$  ng/mL/cc achieving a sensitivity and specificity of 85.7 and 84.4%.

**Discussion**

In this study, the overall rate of PI-RADSV2 category 3 lesions harboring clinically significant PCa was approximately 1 in 10. We identified clinical and imaging features, which were predictive of CSPCa, including higher clinical stage at DRE, higher PSAD and larger MRI lesion

**Clinical and imaging variables to predict diagnosis at targeted biopsy**

size. Overall, these variables performed modestly for predicting CSPCa at targeted biopsy; however, a logistic regression model combining all three variables had high accuracy for diagnosis of CSPCa. This model was particularly useful in the active surveillance cohort within our study. In men undergoing MRI due to persistent clinical suspicion and prior negative template biopsy, PSAD was much more valuable for predicting CSPCa diagnosis at targeted biopsy and had similar high accuracy compared to the logistic regression model.

Higher PSAD has been shown to be a predictor of CSPCa cancer and is a widely evaluated biomarker [4, 7-10, 16, 17]. PI-RADS 3 lesions are indeterminate and currently there is no consensus on the optimal management [5, 6]. It has been proposed that patients with lower PSAD values ( $\leq 0.10 - 0.15$  ng/mL/cc) and PI-RADS category 3 lesions could be safely managed with close surveillance [4, 9, 10]. For example, Gortz et al. found that using a PSAD  $< 0.10$  ng/mL/cc, 43% (43/101) of biopsy naïve men could be spared a biopsy with only 2% (1/43) risk of missing CSPCa [9]. Higher detection rates of CSPCa have been found when stratifying according to higher PSAD values ( $> 0.30$  ng/mL/cc); however, at a risk of missing a proportion of CSPCa [10]. The optimal cut point in patients with persistent high risk after negative biopsy found in our study is higher than the proposed cut points of  $\leq 0.15$  ng/mL/cc [4, 10, 11, 16, 18]. The cut point utilized in clinical practice will need to balance the risk and benefits of potential biopsy with missing a cancer if surveillance is chosen.

Other clinical and imaging biomarkers have shown promise at predicting CSPCa including clinical stage and MR lesion size [7, 8, 11]. Our findings of higher clinical stage in patients with CSPCa are consistent with the current recommendations that DRE should be offered during the initial risk assessment of a patient with disease [19]. We found that larger tumor size was predictive of any PCa and CSPCa, which is consistent with data demonstrating that larger tumors are associated with more aggressive disease [20, 21]. There are no other studies that have showed an association between category 3 lesions size and cancer diagnosis at biopsy, and other studies that have evaluated PI-RADS 3 lesions found no significant differences in relation to tumor size [7, 8, 11]. The present study had the largest sample size, which may account for the significance results of tumor size; however, the further studies are needed to validate our results. Other features associated with CSPCa including with smaller prostate volume, higher PSA and older age [8, 11] may present as lesions categorized by category 4 or 5 lesions and may have been excluded from our study. We did not evaluate other clinical or imaging features such as PSA kinetics or quantitative diffusion imaging metric and further larger multi-institutional studies evaluating all biomarkers would be of interest to improve detection of CSPCa.

The patient population and indication for MRI has been shown to affect the rates of cancer diagnosis [4, 22]. When evaluating men on AS, our model incorporating the significant features (including clinical stage, PSAD and lesion size) improved the accuracy at determining which patients may have CSPCa at MRI-directed targeted biopsy. However, when evaluating patients with persistent clinical suspicious after negative biopsy, PSAD was the single best feature at

determining malignancy. These findings suggest that the optimal PSAD cut-point will be different between groups. This reasoning is supported by extrapolation of data from the systematic review and metaanalysis by Maggi et al, which found differences in any cancer rates between patients who had previous negative biopsy and biopsy naïve men ( $p < 0.001$ ) [4]. With the increased utilization of MRI, MRI-directed biopsy in biopsy naïve men is being explored, and as the cancer rates differ in this subset of patients [4, 23], further work evaluating clinical and imaging predictive factors by MRI indication is of interest.

There are limitations of our study. Despite the large sample size of PI-RADS category 3 lesions, although the rates of malignancy in our study are comparable to those reported in the literature [4], the number of significant cancers remains small which limits analysis. This was a retrospective analysis from a single tertiary care referral center, which may introduce selection bias into our results. MRI-directed targeted biopsy, the comparator in this study, is limited if the tumor was missed and not adequately sampled. This may have been exacerbated by our targeting method, cognitive fusion, as some literature suggests higher targeting accuracies with software fusion or in-bore MRI guided targeting. Results from the recent prospective FUTURE trial indicate no preferential advantage between any of the aforementioned targeting methods which were all utilized in the recent landmark PROMIS and PRECISION trials assessing targeted biopsy for prostate cancer diagnosis [24-26]. Therefore, even if small differences exist among the various methods of performing targeted prostate biopsy, our results reflect the current state of biopsy in clinical practice with similar results to those obtained using other methods of targeting category 3 lesions.

## Conclusions

Our study demonstrates that among equivocal PI-RADSv2 category 3 lesions, clinically significant PCa are uncommon, occurring in approximately 10% of targeted biopsies. Higher clinical stage at digital rectal examination, higher PSAD and larger tumors size measured on MRI are useful features associated with eventual clinically significant prostate cancer diagnosis at targeted biopsy. In men undergoing MRI for AS, a logistic regression model incorporating all of these features was highly accurate at predicting CSPCa diagnosis and significantly improved accuracy of classification compared to each feature assessed independently. In men with persistent clinical suspicion of PCa and negative prior biopsy, PSAD was more valuable and showed similar high accuracy compared to the logistic regression model for prediction of CSPCa at targeted biopsy. A higher reported cut-point of  $\geq 0.215$  ng/mL/cc optimized accuracy of classification in our study. Large scale prospective evaluation of imaging and clinical variables in all patient populations are required. Models incorporating features described in the present study and in prior studies to improve stratification of category 3 lesions require validation.

## References

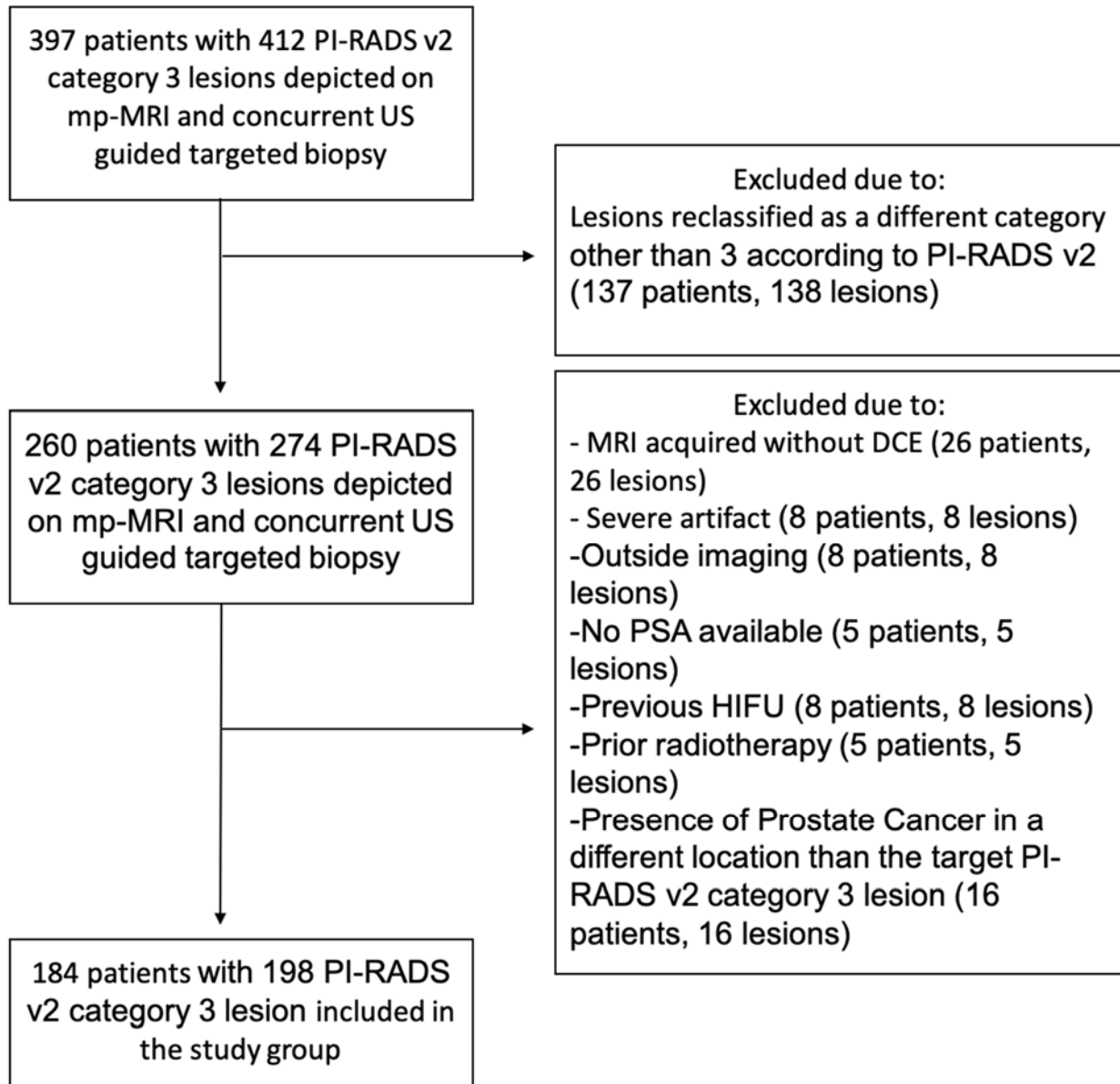
1. Zhang L, Tang M, Chen S, Lei X, Zhang X, Huan Y. A meta-analysis of use of Prostate Imaging Reporting and Data System Version 2 (PI-RADS V2) with multiparametric MR imaging for the detection of prostate cancer. *Eur Radiol* 2017; 27:5204-5214
2. Feng ZY, Wang L, Min XD, Wang SG, Wang GP, Cai J. Prostate Cancer Detection with Multiparametric Magnetic Resonance Imaging: Prostate Imaging Reporting and Data System Version 1 versus Version 2. *Chin Med J (Engl)* 2016; 129:2451-2459
3. Otti VC, Miller C, Powell RJ, Thomas RM, McGrath JS. The diagnostic accuracy of multiparametric magnetic resonance imaging before biopsy in the detection of prostate cancer. *BJU Int* 2019; 123:82-90
4. Maggi M, Panebianco V, Mosca A, et al. Prostate Imaging Reporting and Data System 3 Category Cases at Multiparametric Magnetic Resonance for Prostate Cancer: A Systematic Review and Meta-analysis. *Eur Urol Focus* 2019;
5. Gomez Rivas J, Giganti F, Alvarez-Maestro M, et al. Prostate Indeterminate Lesions on Magnetic Resonance Imaging-Biopsy Versus Surveillance: A Literature Review. *Eur Urol Focus* 2018;
6. Padhani AR, Barentsz J, Villeirs G, et al. PI-RADS Steering Committee: The PI-RADS Multiparametric MRI and MRI-directed Biopsy Pathway. *Radiology* 2019; 292:464-474
7. Felker ER, Raman SS, Margolis DJ, et al. Risk Stratification Among Men With Prostate Imaging Reporting and Data System version 2 Category 3 Transition Zone Lesions: Is Biopsy Always Necessary? *AJR Am J Roentgenol* 2017; 209:1272-1277
8. Sheridan AD, Nath SK, Syed JS, et al. Risk of Clinically Significant Prostate Cancer Associated With Prostate Imaging Reporting and Data System Category 3 (Equivocal) Lesions Identified on Multiparametric Prostate MRI. *AJR Am J Roentgenol* 2018; 210:347-357
9. Gortz M, Radtke JP, Hatiboglu G, et al. The Value of Prostate-specific Antigen Density for Prostate Imaging-Reporting and Data System 3 Lesions on Multiparametric Magnetic Resonance Imaging: A Strategy to Avoid Unnecessary Prostate Biopsies. *Eur Urol Focus* 2019;
10. Washino S, Okochi T, Saito K, et al. Combination of prostate imaging reporting and data system (PI-RADS) score and prostate-specific antigen (PSA) density predicts biopsy outcome in prostate biopsy naive patients. *BJU Int* 2017; 119:225-233
11. Ullrich T, Quentin M, Arsov C, et al. Risk Stratification of Equivocal Lesions on Multiparametric Magnetic Resonance Imaging of the Prostate. *J Urol* 2018; 199:691-698
12. Barentsz JO, Weinreb JC, Verma S, et al. Synopsis of the PI-RADS v2 Guidelines for Multiparametric Prostate Magnetic Resonance Imaging and Recommendations for Use. *Eur Urol* 2016; 69:41-49
13. Zhang M, Milot L, Khalvati F, et al. Value of Increasing Biopsy Cores per Target with Cognitive MRI-targeted Transrectal US Prostate Biopsy. *Radiology* 2019; 291:83-89

## Clinical and imaging variables to predict diagnosis at targeted biopsy

14. Kenigsberg AP, Renson A, Rosenkrantz AB, et al. Optimizing the Number of Cores Targeted During Prostate Magnetic Resonance Imaging Fusion Target Biopsy. *European Urology Oncology* 2018; 1:418-425
15. van der Pol CB, Lee S, Tsai S, et al. Differentiation of pancreatic neuroendocrine tumors from pancreas renal cell carcinoma metastases on CT using qualitative and quantitative features. *Abdom Radiol (NY)* 2019;
16. Schoots IG, Osses DF, Drost FH, et al. Reduction of MRI-targeted biopsies in men with low-risk prostate cancer on active surveillance by stratifying to PI-RADS and PSA-density, with different thresholds for significant disease. *Transl Androl Urol* 2018; 7:132-144
17. Kim TJ, Lee MS, Hwang SI, Lee HJ, Hong SK. Outcomes of magnetic resonance imaging fusion-targeted biopsy of prostate imaging reporting and data system 3 lesions. *World J Urol* 2019; 37:1581-1586
18. Alberts AR, Roobol MJ, Drost FH, et al. Risk-stratification based on magnetic resonance imaging and prostate-specific antigen density may reduce unnecessary follow-up biopsy procedures in men on active surveillance for low-risk prostate cancer. *BJU Int* 2017; 120:511-519
19. Mohler JL, Antonarakis ES, Armstrong AJ, et al. Prostate Cancer, Version 2.2019, NCCN Clinical Practice Guidelines in Oncology. *J Natl Compr Canc Netw* 2019; 17:479-505
20. Lim C, Flood TA, Hakim SW, et al. Evaluation of apparent diffusion coefficient and MR volumetry as independent associative factors for extra-prostatic extension (EPE) in prostatic carcinoma. *J Magn Reson Imaging* 2016; 43:726-736
21. Krishna S, Lim CS, McInnes MDF, et al. Evaluation of MRI for diagnosis of extraprostatic extension in prostate cancer. *J Magn Reson Imaging* 2018; 47:176-185
22. Schoots IG. MRI in early prostate cancer detection: how to manage indeterminate or equivocal PI-RADS 3 lesions? *Transl Androl Urol* 2018; 7:70-82
23. van der Leest M, Cornel E, Israel B, et al. Head-to-head Comparison of Transrectal Ultrasound-guided Prostate Biopsy Versus Multiparametric Prostate Resonance Imaging with Subsequent Magnetic Resonance-guided Biopsy in Biopsy-naive Men with Elevated Prostate-specific Antigen: A Large Prospective Multicenter Clinical Study. *Eur Urol* 2019; 75:570-578
24. Wegelin O, Exterkate L, van der Leest M, et al. The FUTURE Trial: A Multicenter Randomised Controlled Trial on Target Biopsy Techniques Based on Magnetic Resonance Imaging in the Diagnosis of Prostate Cancer in Patients with Prior Negative Biopsies. *Eur Urol* 2019; 75:582-590
25. Ahmed HU, El-Shater Bosaily A, Brown LC, et al. Diagnostic accuracy of multiparametric MRI and TRUS biopsy in prostate cancer (PROMIS): a paired validating confirmatory study. *Lancet* 2017; 389:815-822
26. Kasivisvanathan V, Rannikko AS, Borghi M, et al. MRI-Targeted or Standard Biopsy for Prostate-Cancer Diagnosis. *N Engl J Med* 2018; 378:1767-1777

## Figures and Tables

**Fig. 1.** Flow diagram shows patient selection used in this retrospective study. DCE: dynamic contrast enhancement; HIFU: high intensity focused ultrasound; MP-MRI: multiparametric magnetic resonance imaging; PSA: prostate-specific antigen; US: ultrasound.



## Clinical and imaging variables to predict diagnosis at targeted biopsy

**Fig. 2.** 67-year-old male on active surveillance (AS) with a PI-RADS 3 lesion in the right mid peripheral zone (PZ) yielding clinically significant prostate cancer (CSPCa) Gleason 3+4 (ISUP grade group 2) at targeted biopsy. **(A)** Axial T2-weighted (T2W) magnetic resonance imaging (MRI) shows a non-circumscribed moderately hypointense observation (arrow). **(B)** Axial b 1500 mm<sup>2</sup>/sec diffusion weighted image shows mild-to-moderately high signal intensity in the lesion (arrow). **(C)** Axial apparent diffusion coefficient (ADC) map image shows only corresponding iso- or hypo-intense signal intensity (arrow). **(D)** Subtracted dynamic contrast enhance demonstrate no focal early enhancement, classified as a PI-RADS 3 lesion. White line in **(C)** indicates method of observation size measurement (14 mm) performed on ADC maps for peripheral zone lesions and T2W for transition zone lesions.

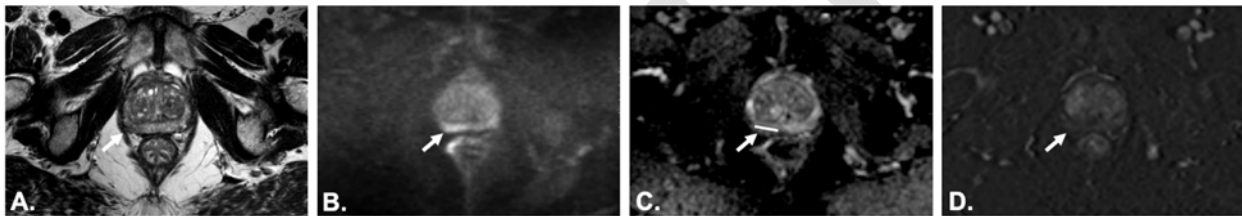
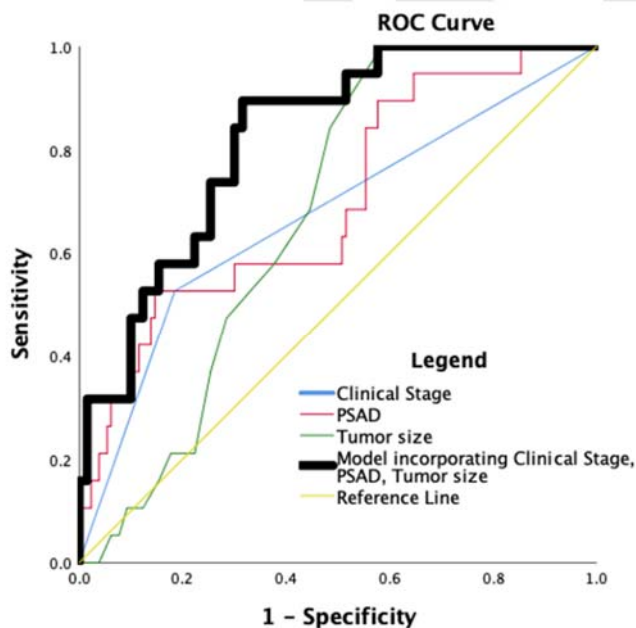


**Fig. 3.** Receiver operator characteristic (ROC) curve depicting accuracy for diagnosis of any significant prostate cancer among PI-RADSV2 assessment category 3 lesions using a logistic regression model combining patient clinical stage, prostate-specific antigen density (PSAD) and larger tumor volume for all patients.



## Clinical and imaging variables to predict diagnosis at targeted biopsy

**Fig. 4.** Receiver operator characteristic (ROC) curve depicting accuracy for diagnosis of any significant prostate cancer among PI-RADSv2 assessment category 3 lesions using a logistic regression model combining patient clinical stage, prostate-specific antigen density (PSAD) and larger tumor volume for patients being managed with active surveillance.

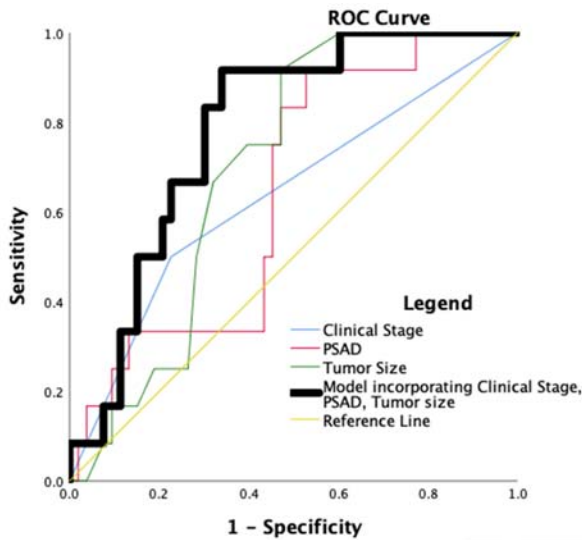


**Fig. 5.** Receiver operator characteristic (ROC) curve depicting accuracy for diagnosis of any significant prostate cancer among PI-RADSv2 assessment category 3 lesions using a logistic regression model combining patient clinical stage, prostate-specific antigen density (PSAD) and larger tumor volume for patients with persistent clinical concern and negative prior biopsy.

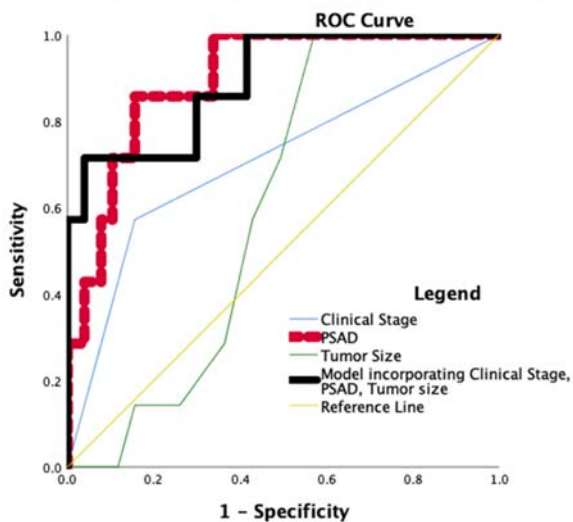


**Table 1. Comparison of categorical and parametric data between PI-RADSv2.1 assessment category 3 lesions with targeted biopsy showing benign, any prostate cancer and significant (ISUP  $\geq 2$ ) prostate cancer in 198 PI-RADS 3 lesions in 184 patients that underwent cognitive fusion MRI-transrectal ultrasound-targeted biopsy**

	<b>Benign histology (n=123)</b>	<b>Any cancer diagnosis (n=61)</b>	<b>p<sup>1</sup></b>	<b>Clinically significant cancer diagnosis (n=20)</b>	<b>p<sup>2</sup></b>
Age (years)	63.1 $\pm$ 8.7	64.0 $\pm$ 7.9	0.484	66.6 $\pm$ 8.2	0.073
PSA <sup>3</sup> (ng/mL)	10.1 $\pm$ 7.1	7.9 $\pm$ 5.0	0.030	10.1 $\pm$ 6.5	0.591
Clinical stage, when available <sup>4</sup>			0.027		0.001
T1c	83.3% (75/90)	67.8% (40/59)		47.4% (9/19)	
$\geq$ T2	16.7% (15/90)	32.2% (19/59)		55.6% (10/19)	
Indication			<0.001		0.023
On AS	26.0% (32/123)	72.1% (44/61)		65.0% (13/20)	
Negative prior biopsy	74.0% (91/123)	27.9% (17/61)		35.0% (7/20)	
Prostate volume (mL)	67.7 $\pm$ 44.1	59.4 $\pm$ 39.4	0.219	49.1 $\pm$ 21.4	0.078
PSA density (ng/mL/cc)	0.171 $\pm$ 0.119	0.163 $\pm$ 0.116	0.630	0.234 $\pm$ 0.151	0.007
Lesion size <sup>5</sup> (mm)	12.4 $\pm$ 5.2	14.0 $\pm$ 5.2	0.047	14.9 $\pm$ 3.3	0.015
Lesion location			0.122		0.023
Peripheral zone	57.8% (78/135)	46.0% (29/63)		30.0% (6/20)	
Transition zone	42.2% (57/135)	54.0% (34/63)		70.0% (14/20)	

<sup>1</sup>Comparison performed between lesions with benign histology and any cancer diagnosis. <sup>2</sup>Comparison performed between lesions with benign and non-significant histology and clinically significant cancer diagnosis. <sup>3</sup>Prostate serum antigen. <sup>4</sup>Total of 149 patient had clinical stage available. Clinical stage compared on a per patient and not per lesions level. <sup>5</sup>Analysis on a per-lesions bases. Total of 135 lesions with benign histology, 43 lesions with ISUP group 1 histology, and 20 with clinically significant ISUP  $\geq 2$  cancer. AS: active surveillance; ISUP: International Society of Urological Pathology; MRI: magnetic resonance imaging; PSA: prostate-specific antigen.

**Table 2. Subgroup analysis for patients on active surveillance and PI-RADSv2.1 assessment category 3 lesions with targeted biopsy showing benign, any prostate cancer and significant (ISUP  $\geq 2$ ) prostate cancer in 82 PI-RADS 3 lesions in 76 patients that underwent cognitive fusion MRI-transrectal ultrasound-targeted biopsy**

	<b>Benign histology (n=36)</b>	<b>Any cancer diagnosis (n=33)</b>	<b>p<sup>1</sup></b>	<b>Clinically significant cancer diagnosis (n=13)</b>	<b>p<sup>2</sup></b>
Age (years)	66.6 $\pm$ 10.2	63.3 $\pm$ 7.9	0.113	66.8 $\pm$ 9.2	0.353
PSA <sup>3</sup> (ng/mL)	9.84 $\pm$ 7.04	7.04 $\pm$ 4.44	0.034	8.56 $\pm$ 6.70	0.800
Clinical stage, when available <sup>4</sup>			0.957		0.056
T1	72.7% (16/22)	72.1% (31/43)		50.0% (6/12)	
$\geq$ T2	27.3% (6/22)	27.9% (12/43)		50.0% (6/12)	
Prostate volume (mL)	75.16 $\pm$ 54.17	60.93 $\pm$ 42.68	0.204	53.26 $\pm$ 21.34	0.263
PSA density (ng/mL/cc)	0.155 $\pm$ 0.097	0.136 $\pm$ 0.079	0.341	0.167 $\pm$ 0.096	0.308
Lesion size <sup>5</sup> (mm)	13.3 $\pm$ 4.9	13.6 $\pm$ 4.9	0.817	15.7 $\pm$ 3.4	0.028
Lesion location <sup>5</sup>			0.418		0.162
Peripheral zone	61.1% (22/36)	52.2% (24/46)		38.5% (5/13)	
Transition zone	38.9% (14/36)	47.8% (20/46)		61.5% (8/13)	

<sup>1</sup>Comparison performed between lesions with benign histology and any cancer diagnosis. <sup>2</sup>Comparison performed between lesions with benign and non-significant histology and clinically significant cancer diagnosis. <sup>3</sup>Prostate serum antigen. <sup>4</sup>Total of 65 patient had clinical stage available. Clinical stage compared on a per patient and not per lesions level. <sup>5</sup>Analysis on a per-lesion bases for a total of 76 lesions. Total of 36 lesions with benign histology, 33 lesions with ISUP group 1 histology, and 13 with clinically significant ISUP  $\geq 2$  cancer. ISUP: International Society of Urological Pathology; MRI: magnetic resonance imaging; PSA: prostate-specific antigen.

**Table 3. Subgroup analysis for patients with negative prior biopsy and PI-RADSv2.1 assessment category 3 lesion with targeted biopsy showing benign, any prostate cancer and significant (ISUP  $\geq 2$ ) prostate cancer in 116 PI-RADS 3 lesion in 108 patients that underwent cognitive fusion MRI-transrectal ultrasound-targeted biopsy**

	<b>Benign histology (n=91)</b>	<b>Any cancer diagnosis (n=17)</b>	<b>p<sup>1</sup></b>	<b>Clinically significant cancer diagnosis n=7)</b>	<b>p<sup>2</sup></b>
Age (years)	61.8 $\pm$ 7.8	65.9 $\pm$ 7.7	0.052	66.1 $\pm$ 6.5	0.206
PSA <sup>3</sup> (ng/mL)	10.2 $\pm$ 7.1	10.3 $\pm$ 5.7	0.975	13.0 $\pm$ 5.2	0.268
Clinical stage, when available <sup>4</sup>			0.005		0.007
T1	86.8% (59/84)	56.3% (9/16)		42.9% (3/7)	
$\geq$ T2	13.2% (9/84)	43.8% (7/16)		57.1% (4/7)	
Prostate volume (mL)	65.04 $\pm$ 40.06	55.56 $\pm$ 29.91	0.356	41.2 $\pm$ 20.7	0.115
PSA density (ng/mL/cc)	0.177 $\pm$ 0.123	0.231 $\pm$ 0.163	0.124	0.360 $\pm$ 0.158	0.0001
Lesion size <sup>5</sup> (mm)	12.1 $\pm$ 5.3	15.0 $\pm$ 5.9	0.038	13.3 $\pm$ 2.7	0.688
Lesion location <sup>5</sup>			0.038		0.036
Peripheral zone	56.6% (56/99)	29.4% (5/17)		14.3% (1/7)	
Transition zone	43.4% (43/99)	70.6% (12/17)		85.7% (6/7)	

<sup>1</sup>Comparison performed between lesions with benign histology and any cancer diagnosis. <sup>2</sup>Comparison performed between lesions with benign and non-significant histology and clinically significant cancer diagnosis. <sup>3</sup>Prostate serum antigen. <sup>4</sup>Total of 84 patient had clinical stage available. Clinical stage compared on a per patient and not per lesion level. <sup>5</sup>Analysis on a per- lesions bases for a total of 116 lesions. Total of 91 lesions with benign histology, 10 lesions with ISUP group 1 histology, and 7 with clinically significant ISUP  $\geq 2$  cancer. ISUP: International Society of Urological Pathology; MRI: magnetic resonance imaging; PSA: prostate-specific antigen.

	<b>Imaging plane</b>	<b>Field of view (mm)</b>	<b>Matrix size</b>	<b>Slice thickness /gap (mm)</b>	<b>TR/TE (msec)</b>	<b>Echo train length</b>	<b>Flip angle</b>	<b>Acceleration factor</b>	<b>Receiver bandwidth (Hz/Voxel)</b>	<b>Approximate acquisition time (min)</b>	<b>Number of signals averaged</b>
T2 TSE <sup>c</sup>	Coronal Sagittal Axial	220x220	320x256	3.0/0 3.0/0 3.0/0	3890– 5250/ 105– 125	27-35	111	N/A	122	4 min 4 min 4 min	1–2
DWI <sup>d</sup>	Axial	220x220	128x80	3.0/0	4200/ 90	1	90	2	1950	5 min	4–15
T1 GRE <sup>f</sup> Dynamic Contrast	Axial	220x220	128x128	3.0/0	4.3/1.3	N/A	12	2	488	5 min	1

<sup>a</sup>Integrated pelvic surface phased-array coils (six channels). <sup>b</sup>Clinical 3 Tesla system: Philips Achieva, Best, the Netherlands. <sup>c</sup>Gradient recalled echo. <sup>d</sup>Turbo/Fast Spin Echo. <sup>e</sup>DWI=Diffusion weighted imaging performed with spectral fat suppression echo planar imaging with tridirectional motion probing gradients and B values of 0 or 100, 400–800 and 1000–1600. Automatic apparent diffusion coefficient map generation and extrapolated images at B values of 1600–2000 were calculated. <sup>f</sup>Dynamic 3D GRE without fat suppression with a temporal resolution of 9–10 seconds after injection of 0.1 mL/kg of gadobutrol (Bayer AG, Leverkusen, Germany) at a rate of 2 mL. MRI: magnetic resonance imaging.